J. Synchrotron Rad. (1998). **5**, 811–813

Thermal and deformation analyses of side-cooled monochromator mirrors for the SPring-8/Figure-8 soft X-ray undulator

Naoto Kihara,* Kiyoto Mashima, Shinnji Miura, Akira Miyaji, Kouichi Wakamiya, Satoshi Takahashi, Motofusa Kageyama and Susumu Ichikawa

Nikon Corporation, Tokyo 140, Japan.
E-mail: kihara@nikongw.nikon.co.jp

(*Received 4 August 1997; accepted 13 December 1997*)

The numerical results for a bent parabolic mirror monochromator designed for the SPring-8/Figure-8 soft X-ray undulator are described. A thermal and structural finite-element analysis is presented for side-cooled premirrors of the bent parabolic mirror monochromator. Using a ray-tracing code, the effect of the final induced figure errors on the performance of the premirror are discussed.

Keywords: thermal finite-element analysis; ray-tracing analysis; SPring-8 photochemistry monochromator; side-cooled mirrors.

1. Introduction

Bent parabolic mirror monochromators (Mashima *et al.*, 1998) require extremely high-quality parabolic mirrors. In order to determine if the proposed design with side-cooled optics performs adequately when subjected to the thermal load of the Figure-8 undulator of SPring-8, precise calculations are required to investigate the thermal load, induced distortion and effect of the final induced figure errors on the performance of the monochromator optics.

When X-rays are absorbed in optical elements, the temperature rises inside the elements. We wanted to determine if the assumption that the heat load on the bent parabolic mirror monochromator on the Figure-8 undulator of SPring-8 would be applied as a surface heat-load flux was correct. Additionally, we wished to investigate whether the degradation of optical performance due to the heat load could be avoided by using water-cooling at the sides of the mirror.

The thermal and optical effects of the Figure-8 undulator power density on a BL-27SU premirror system have been numerically calculated and will be presented below.

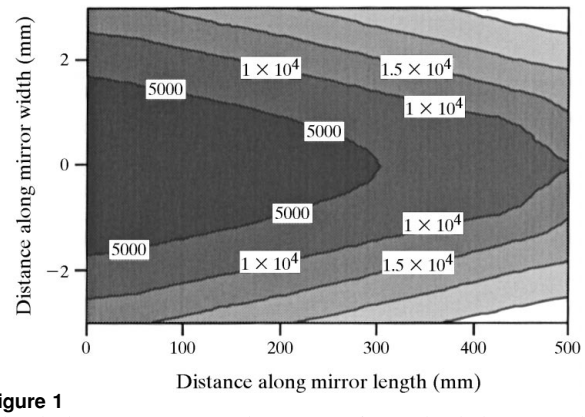

Figure 1
Absorbed power contour of the first premirror. The darkest zone shows power under 5 kW m^{-2}. The lightest zone shows power over 25 kW m^{-2}. *OEHL* concluded that above 99% of the amount of absorbed power is transformed into heat within a 10 μm-thick surface layer.

2. Source and thermal load

The Figure-8 undulator, with an electron beam running at 8.0 GeV, 100 mA stored current for 44 undulator periods of 100 mm length, was modelled with the computer program *SPECTRA* (Tanaka, 1996). The Figure-8 undulator can be considered as a combination of a horizontal and a vertical planar undulator having two deflection parameters, K_x and K_y, respectively (Tanaka & Kitamura, 1995). Deflection parameters K_x = 3.16 and K_y = 3.47 were set, corresponding to an on-axis first peak of 506.2 eV and a total emitted power of 2.94 kW.

This power is directed towards the first horizontally deflecting premirror of the bent parabolic mirror monochromator, which is located 42 m from the source and reflects sideways at a glancing angle of 0.75° to focus the source image on the sample.

The spatial variation of the spectral power distribution has been calculated using *SPECTRA*. The total power absorbed at each point on the surface of the first premirror was taken as the product of the spectral power distribution and the spectral variation of the absorbance ($1 - R$, where R is the reflectivity) of the Pt surface coating.

Using *OEHL* (Tong *et al.*, 1995), the heat load inside the mirror has been computed at each point on the surface using the total absorbed power (the output result of *SPECTRA*). *OEHL* concluded that above 99% of the absorbed power is transformed into heat within 10 μm of the surface layer.

Fig. 1 shows the two-dimensional heat-load contour map of the first premirror. The darkest zone shows power under 5 kW m^{-2} and the lightest zone shows power over 25 kW m^{-2}, corresponding to the projection of the angular dependence of the power density of the Figure-8 undulator.

3. Thermal and deformation models and analyses

Thermal and deformation analyses were carried out applying the commercial finite-element-model (FEM) code *MCS/NASTRAN* (MacNeal–Schwendier Corporation).

3.1. *Thermal model and analysis*

Fig. 2 shows the computer model for the thermal analysis of the side-cooled premirror. The Si bent mirror has a Pt-coated cylindrical surface of 600 mm length, 30 mm width and 45 mm thickness. The opening of the mirror entrance slit restricts the

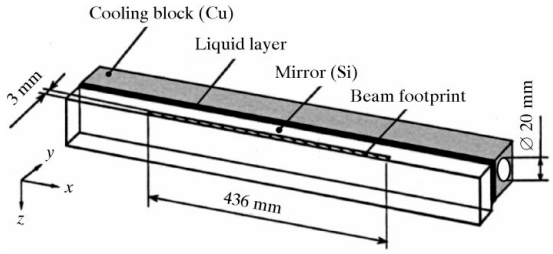

Figure 2
Computer model of the thermal analysis for the side-cooled premirror.

beam footprint on the mirror to 436 mm (length) × 6 mm (width), the total heat load being about 30 W.

The side-cooled system uses a pair of Cu cooling blocks. The water cooling of the Cu blocks was modelled assuming a film coefficient of 1215.05 W m^{-2} K^{-1}, which could be achieved by using a water flow of 0.2 m s^{-1} at 296 K through a 20 mm-diameter duct. The thermal contact conductance at the interface of the liquid Ga layer is assumed to be 3.41 kW m^{-2} K^{-1}, as observed by Asano *et al.* (1992), which could be achieved at a vacuum of 10^{-5} torr and a contact pressure of 284 kPa.

Fig. 3 shows the temperature contour of the side-cooled premirror. The temperature shows an almost homogeneous distribution from 296 to 297 K, which is only 1 K above the cooling temperature.

3.2. *Deformation model and analysis*

Fig. 4 shows the computer model of the deformation analysis for the side-cooled premirror. The cooling blocks are neglected because they are independently supported. A thin layer of liquid metal, which ensures optimal thermal contact, decouples the premirror from the blocks.

This model is assumed to be restrained from vertical motion only at the points *R*. Forces (*F*) act at both ends to bend the mirror into a cylindrical shape. The weight of the mirror is also considered in this model (see *G* in Fig. 4). All the physical parameters are summarized in Table 1.

The results of the FEM calculation for the residual deformation from the elastically bent premirror surface are shown in Fig. 5. The residual deformation is due only to heat load, not to bending. The maximum deformation at the centre of the premirror is 0.25 μm, which corresponds to an averaged slope error of 1 μrad.

4. Effect on optical performance

Fig. 6 shows the focal-spot diagram at the sample located 37 m from the first premirror. We interpolated the deformation data at each mesh point with third-order spline curves in order to perform ray tracing using *Code V* (Optical Research Associates). The radius of the mirror, originally 3000 m, was changed by the deformation and the focal length was shifted by 1.1 m. After readjustment of the focal point, the horizontal focusing spot width on the sample was decreased by about 20%.

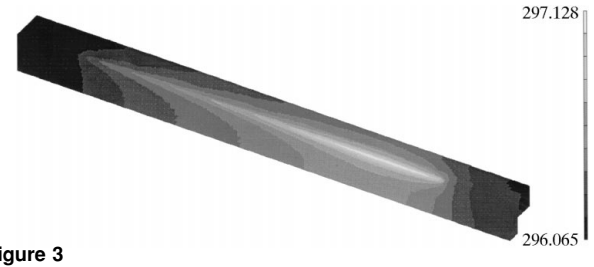

Figure 3
Temperature contour of the side-cooled premirror when the undulator beam hits its top surface. The temperature shows an almost homogeneous distribution from 296 to 297 K.

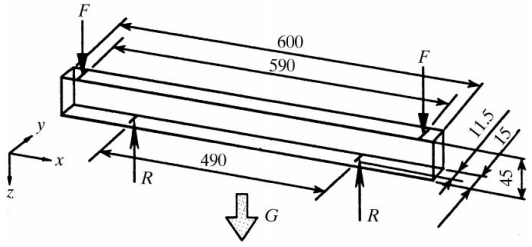

Figure 4
Computer model of the deformation analysis for the side-cooled premirror. Dimensions are in mm.

Table 1
Properties of the material considered for the mirror.

Young's modulus (MPa)	1.308207×10^5
Poisson's ratio	0.27
Mass density (kg m^{-3})	2.33×10^3
Thermal conductivity (W m^{-1} K^{-1})	1.68×10^2
Thermal expansion coefficient	2.33

5. Conclusions and future work

The amount of absorbed power has been calculated using a combination of an undulator code and a heat-energy-deposition code. Taking account of absorption inside the optical element, the calculation shows that, for a Pt-coated Si parabola mirror and a

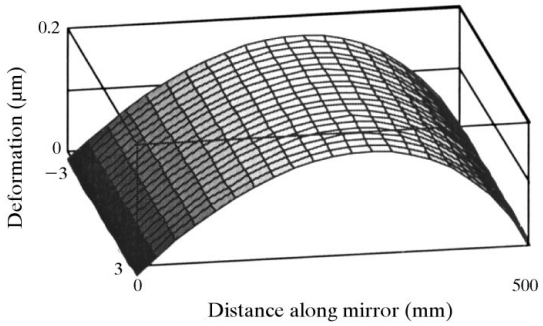

Figure 5
Distortion of the cylindrical premirror surface as a result of the temperature distribution.

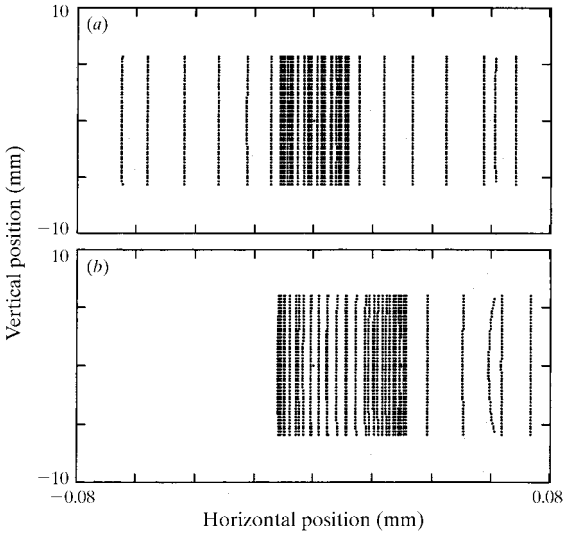

Figure 6
Focal-spot diagram at the sample located 37 m from the premirror. The cylindrical premirror (radius 3000 m) is located 42 m from the source and reflects sideways to focus the source image on the sample. (*a*) The premirror is elastically bent to give a cylindrical surface and focuses the beam with an r.m.s. horizontal spot width of 51 μm. (*b*) The bent premirror is subject to the heat load and focuses the beam with an r.m.s. horizontal spot width of 42 μm.

grazing-incidence angle of 0.75°, above 99% of the absorbed power is transformed into heat within 10 μm of the surface layer.

Finite-element analyses of the temperature variation and thermal distortion were carried out. Combining these analyses and a ray-trace program, it was found that that the on-axis spot diagram alters within 20% in diameter, which is a satisfactory optical performance of the premirror.

This work will be continued to analyse the resulting deformations of the bent parabolic mirrors and grating to assess the optical effect on the high quality of performance of the bent parabolic mirror monochromator.

The authors would like to thank Drs H. Ohashi (JASRI), T. Uruga (RIKEN), T. Motizuki and M. Kuroda (JASRI) for helpful suggestions on *OEHL* analysis and Dr T. Tanaka (RIKEN) for help with the practical aspects of using *SPECTRA*.

References

Asano, M., Ogata, J. & Yoshida, Y. (1992). *Proc. SPIE*, **1739**, 652.
Mashima, K., Kihara, N. & Ishiguro, E. (1998). *J. Synchrotron Rad*. **5**, 817–819.
Tanaka, T. (1996). *SPECTRA Calculation Program for Win/NT*. JAERI-RIKEN SPring-8 Project Team, Spring-8, Kamigori-cho, Hyogo 678-12, Japan.
Tanaka, T. & Kitamura, H. (1995). *Nucl. Instrum. Methods A*, **364**, 368–373.
Tong, X. M., Yamaoka, H. & Nagasawa, H. (1995). *J. Appl. Phys.* **78**(4), 15, 2288–2297.